NASA Technical Memorandum 103749

The Series $Bi_2Sr_2Ca_{n-1}Cu_nO_{2n+4}$ ($1 \leq n \leq 5$): Phase Stability and Superconducting Properties

Mark R. De Guire
Case Western Reserve University
Cleveland, Ohio

Narottam P. Bansal
Lewis Research Center
Cleveland, Ohio

David E. Farrell, Valerie Finan, Cheol J. Kim,
Bethanie J. Hills, and Christopher J. Allen
Case Western Reserve University
Cleveland, Ohio

Prepared for the
91st Annual Meeting of the American Ceramic Society
Indianapolis, Indiana, April 23–27, 1989

NASA

THE SERIES $Bi_2Sr_2Ca_{n-1}Cu_nO_{2n+4}$ ($1 \leq n \leq 5$): PHASE STABILITY AND SUPERCONDUCTING PROPERTIES

Mark R. De Guire*
Case Western Reserve University
Cleveland, Ohio 44106

Narottam P. Bansal
National Aeronautics and Space Administration
Lewis Research Center
Cleveland, Ohio 44135

David E. Farrell, Valerie Finan,
Cheol J. Kim, Bethanie J. Hills,
and Christopher J. Allen
Case Western Reserve University
Cleveland, Ohio 44106

1. ABSTRACT

Phase relations at 850 and 870 °C, and melting transitions in air, oxygen, and helium have been studied for $Bi_{2.1}Sr_{1.9}CuO_6$ and for the series $Bi_2Sr_2Ca_{n-1}Cu_nO_{2n+4}$ for $n = 1, 2, 3, 4, 5$, and ∞ ("$CaCuO_2$"). Up to 870 °C, the $n = 2$ composition resides in the compatibility tetrahedron bounded by $Bi_{2+x}(Sr,Ca)_{3-y}Cu_2O_8$, $(Sr,Ca)_{14}Cu_{24}O_{41}$, Ca_2CuO_3, and a Bi-Sr-Ca-O phase. The $n \geq 3$ compositions reside in the compatibility tetrahedron $Bi_{2+x}(Sr,Ca)_{3-y}Cu_2O_8$-$(Sr,Ca)_{14}Cu_{24}O_{41}$-$Ca_2CuO_3$-CuO up to 850 °C. However, $Bi_{2+x}(Sr,Ca)_{4-y}Cu_3O_{10}$ forms for $n \geq 3$ after extended heating at 870 °C. $Bi_{2+x}Sr_{2-y}CuO_6$ and $Bi_{2+x}(Sr,Ca)_{3-y}Cu_2O_8$ melt in air at 914 and 895 °C respectively. During melting, all of the compositions studied lose 1 to 2 percent by weight of oxygen from the reduction of copper. $Bi_{2+x}Sr_{2-y}CuO_6$, $Bi_{2+x}(Sr,Ca)_{3-y}Cu_2O_8$, and $Bi_{2+x}(Sr,Ca)_{4-y}Cu_3O_{10}$ exhibit crystallographic alignment in a magnetic field, with the c-axes orienting parallel to the field.

2. INTRODUCTION

The discovery by Maeda et al. (ref. 1) of high-temperature superconductivity in the system Bi-Sr-Ca-Cu-O has led to the identification of at least three superconducting compounds in this system. Their structures can be indexed to tetragonal primitive cells with $a = 5.4$ Å, with c increasing as the Ca and Cu contents increase. $Bi_{2.1}Sr_{1.9}CuO_6$ has $T_c \approx 10$ K and $c = 25$ Å. It belongs to a solid solution $Bi_{2+x}Sr_{2-y}CuO_6$, which is reported (refs. 2 to 4) to be distinct from the stoichiometric semiconducting compound $Bi_2Sr_2CuO_6$ or "2201." Hazen et al. (ref. 5) identified a superconductor with the cation stoichiometry (Bi:Sr:Ca:Cu) 2:2:1:2. This phase also belongs to a solid solution (identified as $Bi_2Sr_{3-x}Ca_xCu_2O_8$, with $0.4 < x < 0.9$, by Subramanian et al. (ref. 6)), typically with $80 < T_c < 90$ K and $c = 31$ Å. Finally, $Bi_2(Sr,Ca)_4Cu_3O_{10}$ exhibits $T_c \approx 110$ K and $c = 37$ Å (ref. 7).

Whereas syntheses of nominally phase-pure 25 and 31 Å materials are commonly reported, bulk single-phase 37 Å material is difficult to obtain without dopants (notably Pb) (ref. 8). According to two studies (refs. 9 and 10), the 37 Å phase is

*NASA/ASEE faculty fellow at NASA Lewis Research Center.

not an equilibrium phase at 800 °C in air in the Pb-free Bi-Sr-Ca-Cu-O system. However, one of these studies (ref. 10) found it to be stable at or above 850 °C. It has been reported that the formation of the 37 Å phase can be increased by partial melting (refs. 11 and 12) or by heat treating in reduced p_{O_2} (ref. 13).

The aim of the present work was to resolve some of these issues by studying the subsolidus phase compatibility and the melting relations in $Bi_{2.1}Sr_{1.9}CuO_6$ and in the compositional series $Bi_2Sr_2Ca_{n-1}Cu_nO_{2n+4}$ for n = 1, 2, 3, 4, 5, and ∞ ("$CaCuO_2$"). Prolonged heat treatments were conducted at 850 and 870 °C, followed by phase identification using x-ray diffraction (XRD) and scanning electron microscopy (SEM) with energy-dispersive analysis of x-rays (EDAX). Simultaneous differential thermal analysis (DTA) and thermogravimetric analysis (TGA) were carried out in flowing helium, air, and oxygen to 1100 °C to study the melting behavior in these compositions.

Because the superconducting phases were identified in the present work primarily by XRD, and because of their variable stoichiometries, they will be denoted here as the 25, 31, and 37 Å phases. The samples will be identified by their nominal value of n, with $Bi_{2.1}Sr_{1.9}CuO_6$ denoted as "1'." The nonsuperconducting phases will be denoted by their Bi:Sr:Ca:Cu ratios, with variable Sr/Ca ratios denoted by an x for the Ca stoichiometry, e.g., 0<u>14</u>x<u>24</u> for $(Sr,Ca)_{14}Cu_{24}O_{41}$. Although oxygen contents were not determined in this work, in chemical formulas they will generally be given as simple integers for simplicity.

3. EXPERIMENTAL PROCEDURE

3.1. Sample Synthesis

The binary eutectic at 770±5 °C in the Bi_2O_3-CuO system at 12 to 15 mol % CuO (refs. 14 and 15) makes the present system susceptible to early liquid formation during heating, and to the segregation of liquid to the bottom of the samples. The following procedure was carried out to "tie up" the Bi_2O_3, minimize the free CuO, and to simplify the synthesis of the desired compositions. All heatings were carried out in alumina crucibles. Temperatures were measured by a chromel-alumel thermocouple in contact with the crucibles. Temperatures were constant to ±5 °C throughout all heatings. Grinding was performed by hand in agate or porcelain mortars and pestles. All sample preparations and heating were carried out in air.

"$Bi_2Sr_2O_5$" and "$CaCuO_2$" were synthesized from calculated mixtures of reagent grade Bi_2O_3, $SrCO_3$, $CaCO_3$, and CuO. After 36 hr at 800 °C with two intermediate grindings, powder XRD detected no free Bi_2O_3 or SrO in the "$Bi_2Sr_2O_5$." In the "$CaCuO_2$," however, considerable CaO was still present. Further heating of the latter mixture for 15 hr at 1000 °C, followed by 17 hr at 800 °C, eliminated the CaO and left only the expected (ref. 16) CuO and Ca_2CuO_3.

3.1.1. Synthesis at 800 °C. - CuO was added to the "$Bi_2Sr_2O_5$" to form 2201 (i.e., n = 1) by heating at 800 °C for 20 hr. This was mixed in varying proportions with the "$CaCuO_2$" to make $Bi_2Sr_2Ca_{n-1}Cu_nO_{2n+4}$ with n = 2, 3, 4, and 5. These powders were heated at 800 °C for 45 hr with three intermediate grindings. Powder XRD and DTA/TGA were performed on these samples.

$Bi_{2.1}Sr_{1.9}CuO_6$ was synthesized by first reacting Bi_2O_3 and $SrCO_3$ (with Bi:Sr = 2.1:1.9) at 800 °C for 40 hr with two intermediate grindings. This was then mixed

with the appropriate amount of CuO and heated at 800 °C for 19 hr with one intermediate grinding.

3.1.2. Synthesis at 850 °C. - Portions of the 800 °C powders were heated at 850 °C for 114 hr, followed by furnace cooling at ≈3 °C min^{-1}. These powders were reground and pressed into 13-mm diameter, 1-g pellets at 138 Mpa, which were heated at 850 °C for 15 hr and cooled quickly outside the furnace.

3.1.3. Synthesis at 870 °C. - Portions of the 800 °C powders were pelletized, heated at 870±3 °C for 470 hr with one intermediate grinding, and cooled quickly outside the furnace.

3.2. Characterization

3.2.1. XRD. - Powder XRD (Philips APD 3600 or 3520) was performed using Cu K_α radiation and scan rates of 0.04 to 0.075° s^{-1} over the range $3° \leq 2\theta \leq 60°$. Phases were identified with reference to published powder diffraction patterns of 2201 (refs. 2 to 4 and 17), the 25 Å phase (refs. 2, 3, and 18), the 31 Å phase (refs. 5 and 19), the 37 Å phase (refs. 20 and 21), 014x24 (also called $Sr_3Cu_5O_z$ when x = 0) (refs. 22 and 23), and several Cu-free phases (ref. 23) in addition to the existing JCPDS data (ref. 24) for CuO, 0021, 0201, and 2001.

3.2.2. Thermal analysis. - Simultaneous DTA and TGA (Netzsch STA 429/409) were conducted from room temperature to 1100 °C at a heating rate of 10 °C min^{-1} under flowing helium, air, and oxygen (60 cm^3 min^{-1}). The sample holders were alumina and the reference was alumina powder or an empty alumina sample holder.

3.2.3. Microscopy. - The 870 °C samples were polished using standard procedures, with a final polishing using 0.05 μm alumina powder. These were then examined using a JEOL 840A SEM at 20 keV with a 39 mm working distance. Quantitative cation analysis was performed using a Kevex EDAX unit with an ultra-thin window. Essentially single-phase Bi_2CaO_4, Bi_2CuO_4, and Bi_2SrO_4, synthesized by repeated grinding and heating of the appropriate oxides and carbonates at 800 to 850 °C, were used as reference standards. Spectra were collected for 100 s at a count rate of 10^3 counts s^{-1}. The measured probe currents ranged from 150 to 300 pA. The beam-sample incidence angle was 90° and the x-ray emergence angle was 40°. Many additional semiquantitative analyses were made over wide areas of the samples to confirm that the quantitative analyses reported below were representative of the bulk.

3.2.4. T_c measurements. - Small parallelepipeds ≈2 mm by 2 mm by 10 mm were cut from the pellets. Electrodes were attached to them using silver paint. Four-point resistance measurements from room temperature to 60 K were made with a measuring current of 3 mA.

3.2.5. Magnetic alignment. - An n = 5 sample that had been heated at 870 °C for 70 hr and 850 °C for 15 hr had been found to contain all three superconducting phases. To check for their alignability in a magnetic field, this sample was ground and mixed in an epoxy as in previous work (ref. 25) and exposed at room temperature to a 9.4 T magnetic field for 5 min while the epoxy cured. The degree of crystallographic alignment (c-axis parallel to the field) was determined using an x-ray rocking angle measurement.

4. RESULTS

4.1. 2201 and $Bi_{2.1}Sr_{1.9}CuO_6$

The powder XRD patterns of 2201 and $Bi_{2.1}Sr_{1.9}CuO_6$ (the 25 Å phase) were in excellent agreement with earlier work for their respective phases (refs. 2 to 4), supporting those workers' conclusion that these are distinct phases. No 2201 was detected in the $Bi_{2.1}Sr_{1.9}CuO_6$ XRD pattern. In the 850 °C 2201 sample, the 0$\underline{14}$x$\underline{24}$ phase with x = 0 ($Sr_3Cu_5O_z$ (ref. 22) or $Sr_{14}Cu_{24}O_{41}$ (refs. 26 and 27)) was detectable using XRD, in agreement with the slight copper deficiency of 2201 reported by Ikeda et al. (ref. 3) and Roth et al. (ref. 4). 2201 was semiconducting, with resistance at 15 K approximately 100 times its room temperature value.

The DTA traces for these compounds exhibited endothermic transitions ranging from 850 °C in helium to 925 °C in oxygen (figs. 1 to 3). The peak temperatures in air and helium were 10 to 15 °C higher for the 25 Å phase than for 2201 (table I). The 869 °C shoulder in air in the n = 1 trace may be a eutectic with 0$\underline{14}$x$\underline{24}$. The absence of transitions between the main transitions (914 °C for 1' and 904 °C for n = 1 in air) and 1100 °C suggests that these are the liquidus temperatures for these compositions, consistent with the report of Chakoumakos et al. (ref. 17) that compositions near 2201 were completely liquid at 950 °C. However, further study is needed to elaborate the details of the melting transitions.

4.2. High-T_c Compositions: $2 \leq n \leq 5$ — Phase Analysis

All samples with $2 \leq n \leq 5$ were multiphase. Although the 31 Å phase dominated the XRD patterns of the 850 °C samples, CuO and 0021 were present for $n \geq 3$, increasing with increasing n. (0021 is one endpoint of the 02x1 solid solution, but in the present work the Sr content of this phase was always very low, consistent with the results of other groups (refs. 5, 9, and 10).) Our XRD work on the 0$\underline{14}$x$\underline{24}$ solid solution series (ref. 28) indicates that this phase was also present in the $2 \leq n \leq 5$ series at 850 °C, although it was difficult to identify because of peak overlaps with the other phases.

There was no XRD evidence of the 37 Å phase in the 850 °C samples. This was corroborated by the resistivity measurements (fig. 4(a)), which were virtually identical for n = 2, 3, 4, and 5, with a single resistivity drop centered at 80 K.

In the 870 °C samples, the presence of the 31 Å phase, 0021, and 0$\underline{14}$x$\underline{24}$ was confirmed for $n \geq 3$ using XRD (fig. 5) and EDAX (fig. 6, table II). The proportion of the 31 Å phase (the light-colored matrix phase in fig. 6) decreased from greater than ≈90 percent for n = 2 to ≈50 percent for n = 5, while 0021 and 0$\underline{14}$x$\underline{24}$ increased. The EDAX results for the 31 Å phase for n = 2 and 3 (table II) confirmed that it was Bi-rich and (Sr+Ca)-deficient relative to the 2212 composition. This was consistent with the solid solution range reported by Hong and Mason (ref. 29) at 860 °C.

Unlike the 850 °C results, CuO was undetectable via XRD in the 870 °C samples (fig. 5). Neither could it be detected via SEM/EDAX for n = 3. However, it was found in the n = 5 sample, occasionally as isolated, cracked grains, but primarily as ≈5-μm inclusions in the 0$\underline{14}$x$\underline{24}$ grains (fig. 6(d)). The 0021 phase also frequently occurred as inclusions in the 0$\underline{14}$x$\underline{24}$ grains (fig. 6).

In addition to the Bi-free and 31 Å phases, the XRD patterns of the 870 °C samples (fig. 5) showed an increasing amount of the 37 Å phase with increasing n. This can be seen most clearly by noting the increasing intensities at 24° and 26° (refs. 20 and 21) and the decreasing peak intensities at 2θ = 23° and 25° (refs. 5 and 19). No distinct regions of ≈2:2:2:3 stoichiometry could be detected in the SEM/EDAX studies. However, the composition of the light-colored matrix phase was distinctly shifted to higher Ca contents and Cu/Bi ratios for n = 5, to a composition between (2+x):(3-y):y:2 and (2+x):(4-y):y:3 (table II). This indicates that the matrix contained intergrowths of the 31 and 37 Å phases that were not resolved in the micrographs. Note that if two of the matrix regions in the n = 5 sample were assumed to be only the 31 Å phase, the EDAX results would indicate them to be Bi-deficient (table II), contrary to the earlier results.

Consistent with the phase analysis results, the resistivity measurements of the 870 °C samples (fig. 4(b)) showed two transitions at 80 and 110 K for $n \geq 3$. The latter transition, indicating the 37 Å phase, became larger with increasing n.

In addition to the phases discussed above, XRD detected a phase that was absent for n = 1 (indicating that it contained Ca), was prevalent for $n \geq 2$ at 800 °C, and that diminished with increasing n and temperature. Some characteristic interplanar spacings (and approximate normalized x-ray powder intensities) of this phase were 4.88 Å (25), 4.42 Å (25), 2.991 Å (100), 2.96 Å (100), 2.090 Å (50), and 1.732 Å (25) (ref. 30). These are similar to the XRD patterns of a phase that has been identified as 9<u>11</u>50 (ref. 9) and 24x0 (ref. 23). Majewski et al. (ref. 10) reported a 23x0 phase but gave no diffraction pattern; Roth et al. (ref. 31) identified 23x0 and 2310 as separate solid solution phases. In multiphase samples, it is difficult to pinpoint the stoichiometry of this phase via XRD because several Cu-free phases exhibit their strongest lines at 2θ = 30±1° (refs. 18 and 23).

Lee et al. (ref. 23) reported finding a small amount of 24x0 at 850 °C for n = 2. Our XRD results corroborated this identification. The XRD evidence for a Cu-free phase was weaker in the 870 °C n = 2 sample (peaks marked with an asterisk in fig. 5(a)), but SEM/EDAX revealed a few large (10 to 15 μm) essentially Cu-free grains, slightly darker than the matrix. One of these analyzed as $Bi_2(Sr_{0.45}Ca_{0.52}Cu_{0.03})_{2.90}O_{6-z}$ (fig. 6(a), table II), closer to the 23x0 stoichiometry than to 24x0. Although weak peaks at 2θ = 30° were also visible in the 870 °C samples with $n \geq 3$ (figs. 5(b) to (d)), an extensive EDAX search detected no Cu-free phases in these samples.

4.3. $2 \leq n \leq 5$ — Thermal Analysis

All the compositions studied exhibited multiple endothermic transitions above 870 °C in air. Compared to air, similar transitions occurred at temperatures 15 to 50 °C lower in helium and 10 to 40 °C higher in oxygen, in agreement with the earlier reports (refs. 12 and 13).

The DTA traces for $2 \leq n \leq 5$ all contained a main peak, which occurred at average values of 852±4 °C in helium, 895±3 °C in air, and 908±1 °C in oxygen (table I). Given that the 31 Å phase was a major phase in these compositions, we infer that this main transition involves the 31 Å phase. Its composition independence indicates that it represents either a peritectic or eutectic reaction. In either case, the resulting liquid has a composition near 2212, based on the weakness of the subsequent

transitions in the n = 2 traces. The value of 895±3 °C in air agrees well with the melting point of 885±10 °C for $Bi_4Sr_3Ca_3CuO_4O_{16+x}$ reported by Tarascon et al (ref. 32).

Above the main peak, another peak or shoulder is evident at average values of 879±4 °C in helium, 919±6 °C in air, and 950±9 °C in oxygen. These temperatures are not too different from the main peak temperatures in the n = 1 traces (table I). This suggests that for compositions with $n \geq 2$, the 25 Å phase may be formed as a result of the large melting transition and that the shoulder at higher temperatures arises from melting of this phase.

Finally, a well-resolved peak appeared at higher temperatures (950 to 980 °C in air). This transition shifted steadily to higher temperatures with increasing n. It intensified with increasing n, suggesting that it involves the melting of one of the Bi-free phases. Based on existing data from the binary CaO-CuO and SrO-CuO systems (refs. 16 and 33), 0$\underline{14}$x$\underline{24}$ is a likely candidate: the x = 0 end member has been reported to melt incongruently in air at 955±5 °C (ref. 33), the lowest melting point of the binary alkaline earth cuprates.

Weight losses of a few percent accompanied the melting transitions. These were much larger than, and different from the oxygen exchanges of <1 percent that occur at lower temperatures (ref. 28) and which have been associated with changes of T_c (refs. 11 and 29). The observed weight changes were generally largest and irreversible under helium, and smallest and partially reversible under oxygen, indicating that they resulted from oxygen evolution. The largest fraction of the oxygen loss coincided with the main endothermic peaks, and generally increased with increasing n. The total oxygen loss also increased with increasing n, with a separate oxygen loss, associated with the highest-temperature transition, becoming evident for n = 5. This indicates that the total weight changes were related to the reduction of copper during melting, in the superconducting phases and in the Bi-free compound(s).

4.4. n = ∞ — Thermal Analysis

The n = ∞ sample ("$CaCuO_2$"), which consisted of Ca_2CuO_3 and CuO, showed no thermal activity in air until 1000 °C. There, an endothermic shoulder coincided with the reaction (ref. 16) between CuO and some of the 0021 to form 0012. The subsequent strong endotherms at 1029 and 1054 °C were each accompanied by a 1.85 percent weight loss (0.15 oxygen atoms per $CaCuO_2$ formula unit per peak). These are most likely the result of the incongruent melting of 0012 and/or 0021 with oxygen loss, and the reduction of any remaining CuO to Cu_2O.

4.5 Magnetic Alignment

Like $YBa_2Cu_3O_{7-x}$ (ref. 25) and the Tl-Ba-Ca-Cu oxides (ref. 34), the three Bi-Sr-Ca-Cu-O superconducting phases aligned in an applied magnetic field with their Cu-O planes perpendicular to the field at room temperature. This is demonstrated in figure 7, an XRD pattern of the aligned powder/epoxy composite, taken such that the normal to the diffracting surface was parallel to the field direction. The pattern shows only the 00L-type peaks of the superconducting phases (along with smaller peaks from CuO and 0$\underline{14}$x$\underline{24}$). An x-ray rocking angle measurement of this sample gave a full width at half maximum of 6.5°, indicating that a large fraction of well-aligned grains was present. We note that neither of these x-ray measurements can exclude the

possibility that a significant amount of unaligned material is present. (Pole figure analysis would be required to quantify the degree of alignment more completely.) However, the present data do establish that even multiphase material must contain substantial regions in which all the phases share a common c-axis.

5. DISCUSSION

5.1 Microstructure and Phase Compatibility

Noting that neither XRD or EDAX detected CuO for $n = 2$, we conclude that this composition resides in the compatibility tetrahedron, identified by Hong et al. (ref. 9), bounded by the 31 Å phase, 0$\underline{41}$x$\underline{24}$, 0021, and a Cu-free phase, up to at least 870 °C (fig. 5(a)). The compositions with $n \geq 3$, on the other hand, exist in the tetrahedron of CuO, 0021, 0$\underline{41}$x$\underline{24}$, and the 31 Å phase (ref. 9) up to 850 °C. (It is interesting to note that Hazen et al, (ref. 5) observed these four phases in their early characterization of a polyphase $BiSrCaCu_3O_z$ material.) This also corroborates the finding that the 31 Å phase, like the 25 Å phase (refs. 2,3,12, and 18), tends to be Bi-rich or (Sr+Ca)-deficient compared to the idealized composition; if its stoichiometry were 2212, the $2 \leq n \leq 5$ compositions would lie entirely in the three-phase region formed by 2212, CuO, and 0021 (refs. 9 and 10).

The SEM results show that the 0$\underline{14}$x$\underline{24}$ phase (the lighter of the two dark phases in figs. 6(a) to (d)) was invariably surrounded by the superconducting matrix, often in the form of a thin (1-μm) coating, maintaining close contact with it along sharply faceted grain boundaries. This contrasts with the tangled, spaghetti-like arrangement of the superconductor that predominates throughout the matrix. This microstructure implies that an epitaxial relationship exists between 0$\underline{14}$x$\underline{24}$ and the superconducting phase(s), perhaps related to the structural similarities observed by McCarron et al. (ref. 19).

The broad superconducting transitions, low $T_{c,0}$ values, and the flat normal-state resistivity of the $n = 3$, 870 °C sample (fig. 4) may result from the presence of the nonsuperconducting phases. In general, however, the interconnected, plate- and needle-like morphology of the superconducting matrix (fig. 6) enabled it to maintain electrical continuity, even as it decreased in proportion to the Bi-free compounds. It may prove advantageous to exploit this tendency by fabricating in-situ composites, with the size and distribution of the nonsuperconducting phases optimized to improve flux pinning, impurity gettering, and (ultimately) critical current density. However, in preliminary studies on the $2 \leq n \leq 5$ series with a Bi/Sr ratio of 2.1/1.9 (like the 1' sample reported here), the relative proportions of the super- and semiconducting phases were unchanged, but the interconnectivity of the matrix was lost for $n \geq 4$, and the samples behaved overall as semiconductors.

The coexistence of five solid phases (02x1, 0$\underline{14}$x$\underline{24}$, CuO, and the 31 and 37 Å phases) in the 870 °C $n = 5$ sample implies a nonequilibrium situation. The appearance of the 37 Å phase at the expense of the 31 Å phase indicates that the former, and not the latter, is stable above 850 °C for large n. However, the higher-T_c phase forms very slowly from the 31 Å phase and one or more of the Bi-free phases, such that five phases persisted even after 470 hr with one intermediate grinding. These findings agree with the conclusions of Majewski et al. (ref. 10).

5.2 Thermal Analysis

It is natural to look in the DTA results for evidence of the formation of the 37 Å phase. The main 895 °C peak was preceded by a shoulder near 874 °C for $n = 2$ and $n = 3$ in air. Although this coincides with the temperature of the 37 Å phase formation, this shoulder cannot account for the increasing degree of 37 Å phase formation with increasing n. The $n = 2$ and $n = 3$ 870 °C samples contained none and little 37 Å phase respectively, whereas the $n = 4$ and $n = 5$ compositions, which exhibited no shoulder, formed substantial amounts of the 37 Å phase. We note that the DTA trace of reportedly single-phase $Bi_4Sr_3Ca_3Cu_4O_{16+x}$ in air (ref. 32) exhibits all of the same features as the present $n = 2$ and $n = 3$ traces in figure 2 except for the 874 °C shoulder, and this composition also formed the 37 Å phase on heating at 870 °C. It is likely that the 874 °C shoulder arises from one or more reactions that consume the Cu-free phase and CuO, which were observed as minor phases in the 850 °C samples but were further diminished in the 870 °C samples.

Considering the extreme sluggishness of the formation of the 37 Å phase, this reaction would not be expected to show up in the DTA traces. As a result, the observed DTA transitions for $n > 2$ are probably metastable extensions of the reactions that occur for $n = 2$, i.e., the reactions that would be observed in the absence of the 37 Å phase.

It should also be pointed out that the appearance of the 37 Å phase at 870 °C in air, appreciably below the lowest-temperature DTA transitions for $n \geq 3$, argues for a purely solid-state reaction. While Pb additions and lower oxygen partial pressures may achieve accelerated 37 Å phase formation by promoting liquid phase formation, it appears that the 37 Å phase is stable in the subsolidus region. Syntheses that avoid formation of the 31 Å phase, for example by rapid heating to 870 °C of an intimately mixed, homogeneous Ca- and Cu-rich composition, could conceivably achieve T_c's of 110 K in a single, more rapid reaction.

Figures 5 and 6 showed that increasing n beyond 3 increases the proportion of the 37 Å phase, even while the overall composition moves away from the superconductor toward the Bi-free phases. Shi et al. (ref. 35) reported similar results in Bi-Sr-Ca-Cu-O glass ceramics. They inferred that the excess Ca and Cu accelerate the formation of the 37 Å phase. An alternative explanation is that the presence of greater quantities of 0021 and 0$\underline{14}$x$\underline{24}$ impedes the formation of the slow-to-transform 31 Å phase, allowing the 37 Å phase to form directly from compounds that react more readily.

Regarding the transitions above the main 895 °C reaction, we note that Gazit et al. (ref. 36) and Haggerty et al. (ref. 37) identified a 0$\underline{14}$x$\underline{24}$ composition as the solid present just before solidification of the 31 Å phase in laser float zone crystal growth experiments. Their results are not necessarily inconsistent with the present interpretation (i.e., the 25 Å phase forming between 0$\underline{14}$x$\underline{24}$ and the 31 Å phase), because they reported often observing the 25 Å phase in multiphase regions of their as-solidified materials. We have frequently observed the 25 and 31 Å phases to grow side by side, and presumably epitaxially, during similar experiments (ref. 38), indicating that they coexist at some stage of the solidification process.

6. SUMMARY OF RESULTS

A shared characteristic of the superconducting phases in the Bi-Sr-Ca-Cu-O system is Bi excess and Sr (or Sr+Ca) deficiency, relative to the originally proposed 2:2:0:1, 2:2:1:2, and 2:2:2:3 compositions. $Bi_2Sr_2CuO_6$ is a semiconductor with an XRD pattern and melting temperature different from those of the low-temperature superconductor $Bi_{2.1}Sr_{1.9}CuO_6$. The compositions $Bi_2Sr_2Ca_{n-1}Cu_nO_{2n+4}$ for $2 \leq n \leq 5$ are multiphase. The $n = 2$ composition at 850 to 870 °C consists mostly of $Bi_{2.2}Sr_{1.3}Ca_{1.2}Cu_2O_8$ (the 31 Å phase), with small amounts of Ca_2CuO_3, $(Sr,Ca)_{14}Cu_{24}O_{41}$, and a Cu-free phase of $Bi_2(Sr,Ca)_4O_7$ or $Bi_2(Sr,Ca)_3O_6$ stoichiometry. The compositions with $n \geq 3$ consist of $Bi_{2+x}(Sr,Ca)_{3-y}Cu_2O_6$, $(Sr,Ca)_{14}Cu_{24}O_{41}$, Ca_2CuO_3, and CuO at 850 °C. The only superconducting compound stable at 850 °C for $2 \leq n \leq 5$ is the 31 Å phase. Virtually identical resistivity-versus-temperature curves are obtained for these samples, with a single superconducting transition at $T_{c,mid} = 80$ K. At temperatures above 850 °C, $Bi_{2+x}(Sr,Ca)_{4-y}Cu_3O_{10}$, the 37 Å phase, becomes stable for $n \geq 3$. However, its formation is so sluggish that it exists only as intergrowths with the 31 Å phase, in a continuous superconducting matrix that surrounds the grains of $(Sr,Ca)_{14}Cu_{24}O_{41}$, Ca_2CuO_3, and CuO. Two superconducting transitions at 80 and 110 K result, with the magnitude of the drop at 110 K increasing with increasing n.

The 25 Å phase melts at 914 °C in air. The 31 Å phase melts at 895 °C. The latter reaction may result in the formation of the 25 Å phase, which subsequently melts to form $(Sr,Ca)_{14}Cu_{24}O_{41}$ at higher temperatures. All of the melting reactions are accompanied by oxygen losses of up to 2 percent, which are associated with the reduction of copper in the superconducting phases and the Bi-free phases.

The three superconducting phases exhibit crystallographic alignment in a magnetic field, such that the c-axis orient parallel to the field.

7. CONCLUSIONS

It may be concluded that the 25 and 31 Å superconducting phases are Bi-rich or (Sr+Ca)-deficient rather than having the ideal stoichiometric 2201 and 2212 compositions, respectively. Also, the kinetics of formation of the high-T_c (37 Å) phase from the 31 Å phase and one or more of the Bi-free phases is extremely sluggish.

8. ACKNOWLEDGMENTS

This work was supported by the NASA/ASEE summer faculty fellowship to Mark De Guire at NASA Lewis. The authors thank Ralph Garlick for performing XRD runs and Anna Palczer and Joseph Wagner for DTA/TGA analysis.

REFERENCES

1. H. Maeda, Y. Tanaka, M. Fukutomi, and T. Asano, Jpn. J. Appl. Phys. **27** [2] L209-L210 (1988).

2. J.A. Saggio, K. Sujata, J. Hahn, S.J. Hwu, K.R. Poeppelmeier, and T.O. Mason, J. Am. Ceram. Soc. **72** [5] 849-853 (1989).

3. Y. Ikeda, H. Ito, S. Shimomura, Y. Oue, K. Inaba, Z. Hiroi, and M. Takano, Physica C **159** [1] 93-104 (1989).

4. R.S. Roth, C.J. Rawn, and L.A. Bendersky, J. Mater. Res. **5** [1] 46-52 (1990).

5. R.M. Hazen, C.T. Prewitt, R.J. Angel, H.L. Ross, L.W. Finger, C.G. Hadidiacos, D.R. Veblen, P.J. Heaney, P.H. Hor, R.L. Meng, Y.Y. Xue, Y.Q. Wang, Y.Y. Sun, Z.J. Huang, L. Gao, J. Bechtold, and C.W. Chu, Phys. Rev. Lett. **60** [12] 1174-1177 (1988).

6. M.A. Subramanian, C.C. Torardi, J.C. Calabrese, J. Gopalakrishnan, K.J. Morrissey, T.R. Askew, R.B. Flippen, U. Chowdhry, and A.W. Sleight, Science **239**[4843] 1015-1017 (1988).

7. J.M. Tarascon, W.R. McKinnon, P. Barboux, D.M. Hwang, B.G. Bagley, L.H. Greene, G. Hull, Y. LePage, N. Stoffel, and M. Giroud, Phys. Rev. **B38** [13] 8885-8892 (1988).

8. S.A. Sunshine, T. Siegrist, L.F. Schneemeyer, D.W. Murphy, R.J. Cava, B. Battlogg, R.B. van Dover, R.M. Fleming, S.H. Glarum, S. Nakahara, R. Farrow, J.J. Krajewski, S.M. Zahurak, J.V. Waszczak, J.H. Marshall, P. Marsh, L.W. Rupp, Jr., and W.F. Peck, Phys. Rev. **B38** [1] 893-896 (1988).

9. B.-S. Hong, J. Hahn, and T.O. Mason, J. Am. Ceram. Soc. **73** [7] 1965-1972 (1990).

10. P. Majewski, B. Freilinger, B. Hettich, T. Popp, and K. Schulze, to be published in Proceedings of the ICMC '90 Conference on High-Temperature Superconductors—Material Aspects, Garmisch Partenkirchen, FRG, 9-11 May, 1990.

11. J.L. Tallon, R.G. Buckley, P.W. Gilberd, M.R. Presland, I.W.M. Brown, M.E. Bowden, L.A. Christian, and R. Goguel, Nature **333** [6] 153-156 (1988).

12. J. Tsuchiya, H. Endo, N. Kijima, A. Sumiyama, M. Mizuno, and Y. Oguri, Jpn. J. Appl. Phys. **28** [11] L1918-L1921 (1989).

13. U. Endo, S. Koyama, and T. Kawai, Jpn. J. Appl. Phys. **27** [8] L1476-1479 (1988).

14. J.-C. Boivin, D. Thomas, and G. Tridot, C. R. Acad. Sci. Paris **276** [13] 1105-1107 (1973).

15. B.G. Kakhan, V.B. Lazarev, and I.S. Shaplygin, Russ. J. Inorg. Chem. **24** [6] 922-927 (1979).

16. R.S. Roth, C.J. Rawn, J.J. Ritter, and B.P. Burton, J. Am. Ceram. Soc. **72**[8] 1545-1549 (1989).

17. B.C. Chakoumakos, P.S. Ebey, B.C. Sales, and E. Sonder, J. Mater. Res. **4** [4] 767-780 (1989).

18. R.S. Roth, C.J. Rawn, B.P. Burton, and F. Beech, J. Res. Natl. Inst. Stand. Technol. **95** 291-295 (1990).

19. M. Onoda, A. Yamato, E. Takayama-Muromachi, and S. Takekawa, Jpn. J. Appl. Phys. **27** [5] L833-L836 (1988).

20. G. Calestani, C. Rizzoli, G.D. Andreetti, E. Buluggiu, D.C. Giori, A. Valenti, A. Vera, and G. Amoretti, Physica C **158** [1] 217-224 (1989).

21. J.L. Tallon, R.G. Buckley, P.W. Gilberd, and M.R. Presland, Physica C **158** [1-2] 247-254 (1989).

22. H. Kitaguchi, M. Ohno, M. Kaichi, J. Takada, A. Osaka, Y. Miura, Y. Ikeda, M. Takano, Y. Bando, Y. Takeda, R. Kanno, and O. Yamamoto, J. Ceram. Soc. Jpn, **96** 397-403 (1988).

23. C.-L. Lee, J.-J. Chen, W.-J. Wen, T.-P. Perng, J.-M. Wu, T.-B. Wu, T.-S. Chin, R.-S. Liu, and P.-T. Wu, J. Mater. Res. **5** [6] 1403-1409 (1990).

24. X-ray Powder Diffraction File, Joint Committee on Powder Diffraction Standards, Swarthmore, Pennsylvania; Cards # 5-661, 34-282, 34-283, 26-502.

25. D.E. Farrell, B.S. Chandrasekhar, M.R. De Guire, M.M. Fang, V.G. Kogan, J.R. Clem, and D.K. Finnemore, Phys. Rev. B **36** [7] 4025-4027 (1987).

26. E.M. McCarron, III, M.A. Subramanian, J.C. Calabrese, and R.L. Harlow, Mat. Res. Bull. **23** [9] 1355-1365 (1988).

27. T. Siegrist, L.F. Schneemeyer, S.A. Sunshine, J.V. Waszczak, and R.S. Roth, Mat. Res. Bull. **23** [10] 1429-1438 (1988).

28. C.J. Kim, Ph.D. Dissertation, Case Western Reserve Univ., January (1991).

29. B.-S. Hong and T.O. Mason, preprint.

30. M.R. De Guire, V. Finan, and N.P. Bansal, presented at the 91st Annual Meeting of the American Ceramic Society, Indianapolis, Indiana, paper 25-SVI-89, 24 April, 1989.

31. R.S. Roth, B.P. Burton, and C.J. Rawn, Ceram. Trans., **13** 23-24 (1990).

32. J.M. Tarascon, Y. LePage, P. Barboux, B.G. Bagley, L.H. Greene, W.R. McKinnon, G.W. Hull, M. Giroud, and D.M. Hwang, Phys. Rev. **B37** [16] 9382-9389 (1988).

33. N.M. Hwang, R.S. Roth, and C.J. Rawn, J. Am. Ceram. Soc. **73** [8] 2531-2533 (1990).

34. D.E. Farrell, C.M. Williams, S.A. Wolf, N.P. Bansal, and V.G. Kogan, Phys. Rev. Lett. **61** [24] 2805-2808 (1988).

35. D. Shi, M. Blank, M. Patel, D.G. Hinks, A.W. Mitchell, K. Vandervoort, and H. Claus, Physica C **156** [5] 822-826 (1988).

36. D. Gazit, P.N. Peszkin, L.V. Moulton, and R.S. Feigelson, J. Cryst. Growth **98** [3] 545-549 (1989).

37. H.M. Chow, X.P. Jiang, M.J. Cima, J.S. Haggerty, H.D. Brody, and M.C. Flemings, to be published in the Proc. MRS Symp., Fall 1989.

38. C.J. Kim, M.R. De Guire, C.J. Allen, and A. Sayir, Mater. Res. Bull. 26 [1] 29-39 (1991).

TABLE I. - SUMMARY OF PEAK TEMPERATURES AND WEIGHT LOSSES DURING SIMULTANEOUS DTA/TGA OF $Bi_2Sr_2Ca_{n-1}Cu_nO_{2n+4}$

[Heat rate: 10 °C/min; atmosphere flow rate: 60 cm^3 min^{-1}; s denotes a shoulder on a larger peak.]

n	Helium		Air		Oxygen	
	Peak T, °C	Weight loss, percent	Peak T, °C	Weight loss, percent	Peak T, °C	Weight loss, percent
[a]1'	878(s) 900	1.44	907(s) 914	1.06	---------- 922	---- 1.08
1	845(s) 875(s) 886	0.93	869(s) 890(s) 904	---- ---- .22	---------- ---------- 923	---- ---- .47
2	845(s) 856 880(s) 901(s)	2.42 ---- ----	872(s) 895 925(s) 953	1.24 ---- ----	---------- 907 941 982	---- 1.29
3	840(s) 856 883(s) 892	3.06	876(s) 892 920(s) 954	1.49 ---- ----	---------- 908 923,949(s) 980	---- 1.76
4	853 877(s) 894	3.22	898 913(s) 968	---- ---- ----	909 952(s) 991	1.94
5	848 875(s) 895	2.1 1.7	895 920(s) 981	2.0 .9	907 947(s),959 1001	1.6 0.5
∞	------ ------ ------	---- ---- ----	1000(s) 1029 1054	---- 1.85 1.84	---------- ---------- ----------	---- ---- ----

[a] $Bi_{2.1}Sr_{1.9}CuO_{6\pm z}$

TABLE II. - SUMMARY OF EDAX RESULTS FROM FIGURE 6

n	Cation, percent[a]				Stoichiometry	Region
	Bi	Sr	Ca	Cu		
2	32.8	19.8	16.8	30.6	$Bi_{2.15}Sr_{1.30}Ca_{1.10}Cu_2O_{8-z}$	1
	33.2	18.4	18.3	30.1	$Bi_{2.20}Sr_{1.22}Ca_{1.22}Cu_2O_{8-z}$	2
	2.4	4.7	63.1	29.9	$Bi_{0.08}Sr_{0.156}Ca_{2.11}CuO_{3+z}$	3
	3.0	15.5	18.7	62.8	$Bi_{1.14}Sr_{5.92}Ca_{7.16}Cu_{24}O_{41-z}$	4
	40.8	26.7	30.6	1.9	$Bi_2Sr_{1.31}Ca_{1.50}Cu_{0.10}O_{6-z}$	5
3	31.9	18.4	19.6	30.2	$Bi_{2.11}Sr_{1.22}Ca_{1.30}Cu_2O_{8-z}$	1
	33.4	17.2	20.4	29.0	$Bi_{2.30}Sr_{1.18}Ca_{1.40}Cu_2O_{8-z}$	2
	2.4	3.5	65.0	29.2	$Bi_{0.08}Sr_{0.12}Ca_{2.23}CuO_{3+z}$	3
	2.1	3.4	64.9	29.6	$Bi_{0.07}Sr_{0.11}Ca_{2.19}CuO_{3+z}$	4
	2.5	4.4	64.6	28.6	$Bi_{0.08}Sr_{0.15}Ca_{2.26}CuO_{3+z}$	5
	3.6	14.0	21.2	61.3	$Bi_{1.39}Sr_{5.48}Ca_{8.30}Cu_{24}O_{41-z}$	6
	3.4	12.9	23.1	60.8	$Bi_{1.33}Sr_{5.04}Ca_{9.11}Cu_{24}O_{41-z}$	7
	3.0	11.8	25.3	59.9	$Bi_{1.22}Sr_{4.71}Ca_{10.12}Cu_{24}O_{41-z}$	8
5	28.7	15.2	24.2	31.9	$Bi_{1.80}Sr_{0.95}Ca_{1.51}Cu_2O_{8-z}$ or $Bi_{2.70}Sr_{1.43}Ca_{2.27}Cu_3O_{10-z}$	1
	31.3	14.6	21.0	33.1	$Bi_{1.89}Sr_{0.88}Ca_{1.27}Cu_2O_{8-z}$ or $Bi_{2.83}Sr_{1.32}Ca_{1.91}Cu_3O_{10-z}$	2
	30.8	13.7	25.3	30.3	$Bi_{2.03}Sr_{0.90}Ca_{1.67}Cu_2O_{8-z}$	3
	1.9	0.0	68.5	29.6	$Bi_{0.06}Ca_{2.31}CuO_{3+z}$	4
	1.8	3.0	66.5	28.8	$Bi_{0.06}Sr_{0.10}Ca_{2.31}CuO_{3+z}$	5
	3.7	8.8	27.9	59.6	$Bi_{1.49}Sr_{3.54}Ca_{11.25}Cu_{24}O_{41-z}$	6
	3.2	10.2	25.8	60.8	$Bi_{1.26}Sr_{4.04}Ca_{10.19}Cu_{24}O_{41-z}$	7
	3.2	9.5	59.5	27.7	$Bi_{1.3}Sr_{3.8}Ca_{11.2}Cu_{24}O_{41-z}$	8
	2.6	0.0	.4	97.0	CuO	9,10

[a]Uncertainties (±2 σ) from the fitting algorithm ranged from 0.1 to 0.6 cation percent. Additional uncertainties of up to 2 cation percent can arise from the background correction procedure, particularly for Bi and Sr.

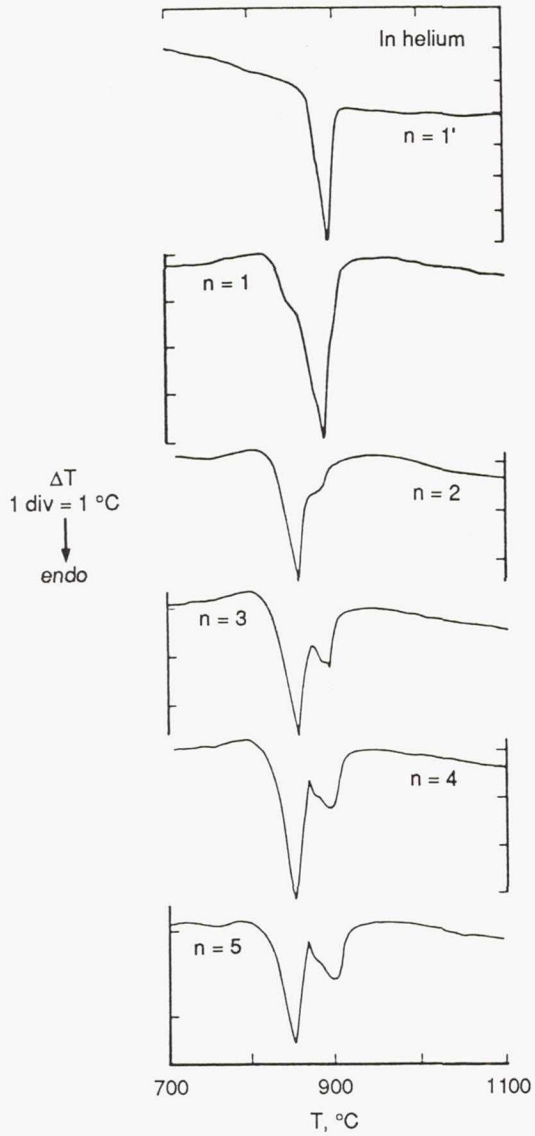

Figure 1.—DTA traces of $Bi_{2.1}Sr_{1.9}CuO_z$ (n = 1', top) and $Bi_2Sr_2Ca_{n-1}Cu_nO_{2n+4}$ with n = 1, 2, 3, 4, and 5. Atmosphere: flowing helium (60 cm^3 min^{-1}). Heating rate: 10 °C min^{-1}. Sample weights: 1': 166.1 mg; 1: 205.9 mg; 2: 94 mg; 3: 133.6 mg; 4: 131.6 mg; 5: 111.2 mg.

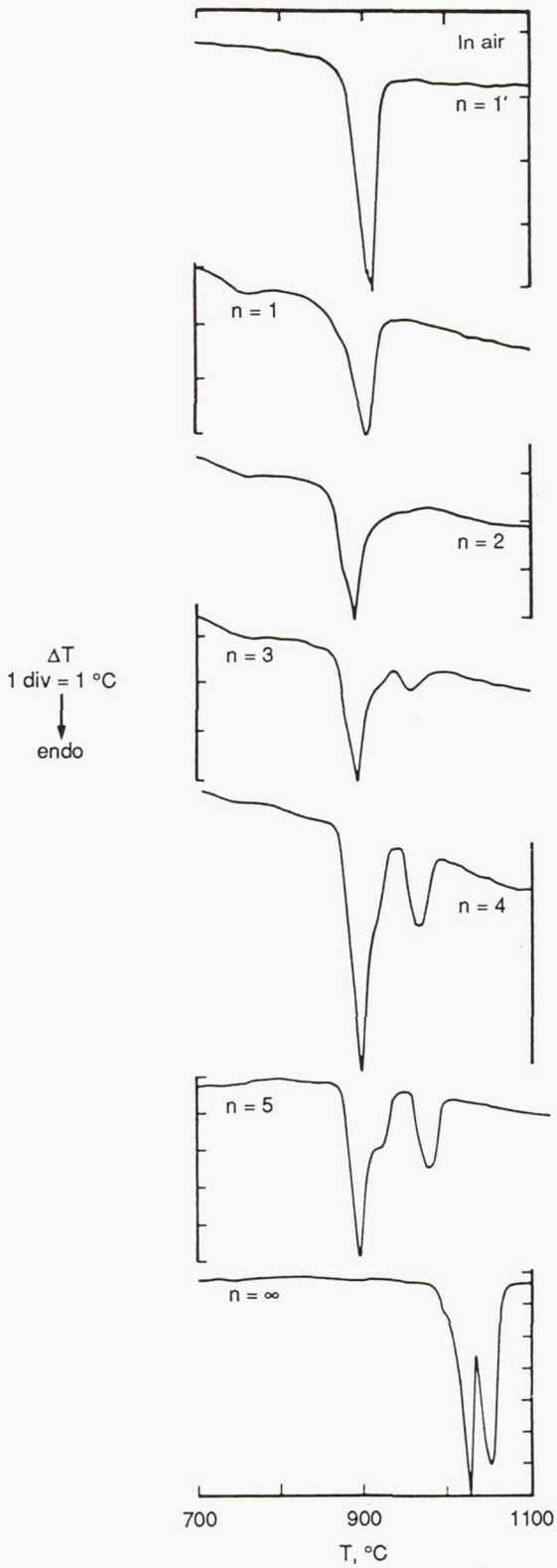

Figure 2.—DTA traces of $Bi_{2.1}Sr_{1.9}CuO_z$ (n = 1', top) and $Bi_2Sr_2Ca_{n-1}Cu_nO_{2n+4}$ with n = 1, 2, 3, 4, 5 and ∞. Atmosphere: flowing air (60 cm^3 min^{-1}). Heating rate: 10 °C min^{-1}. Sample weights: 1': 50.8 mg; 1: 69.5 mg; 2: 65.2 mg; 3: 60.2 mg; 4: 159.1mg; 5: 139.mg; ∞: 136.2mg.

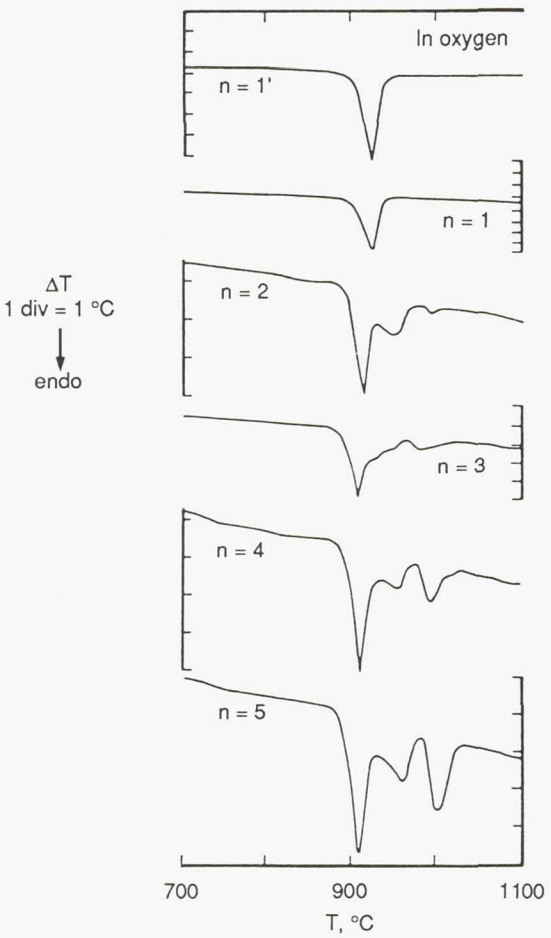

Figure 3.—DTA traces of $Bi_{2.1}Sr_{1.9}CuO_z$ (n = 1', top) and $Bi_2Sr_2Ca_{n-1}Cu_nO_{2n+4}$ with n = 1, 2, 3, 4, and 5. Atmosphere: flowing oxygen (60 cm^3 min^{-1}). Heating rate: 10 °C min^{-1}. Sample weights: 1': 157.8 mg; 1: 133.2 mg; 2: 84.3 mg; 3: 96.6 mg; 4: 96.5 mg; 5: 146.9 mg.

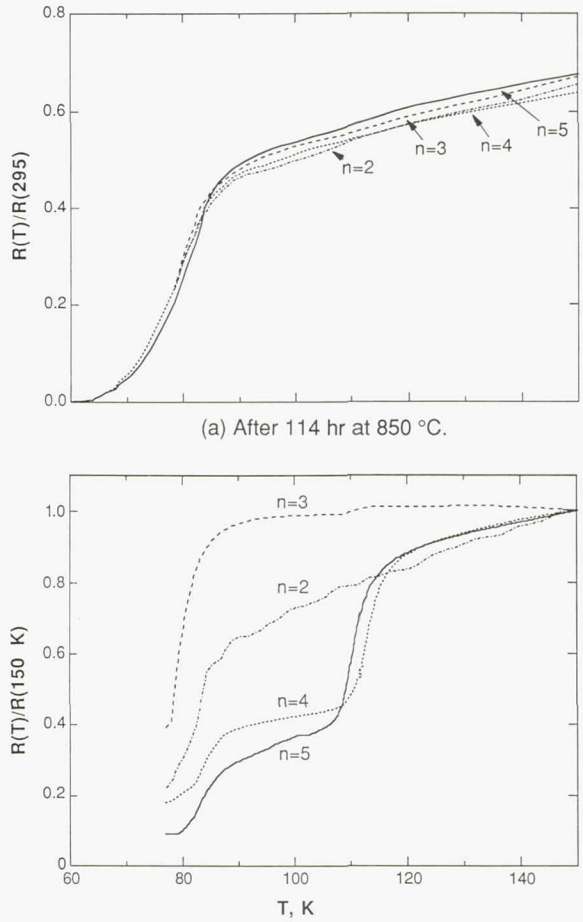

(a) After 114 hr at 850 °C.

(b) After 470 hr at 870 °C.

Figure 4.—Normalized resistance versus temperature curves for the series $Bi_2Sr_2Ca_{n-1}Cu_nO_{2n+4}$ (n = 2, 3, 4, and 5).

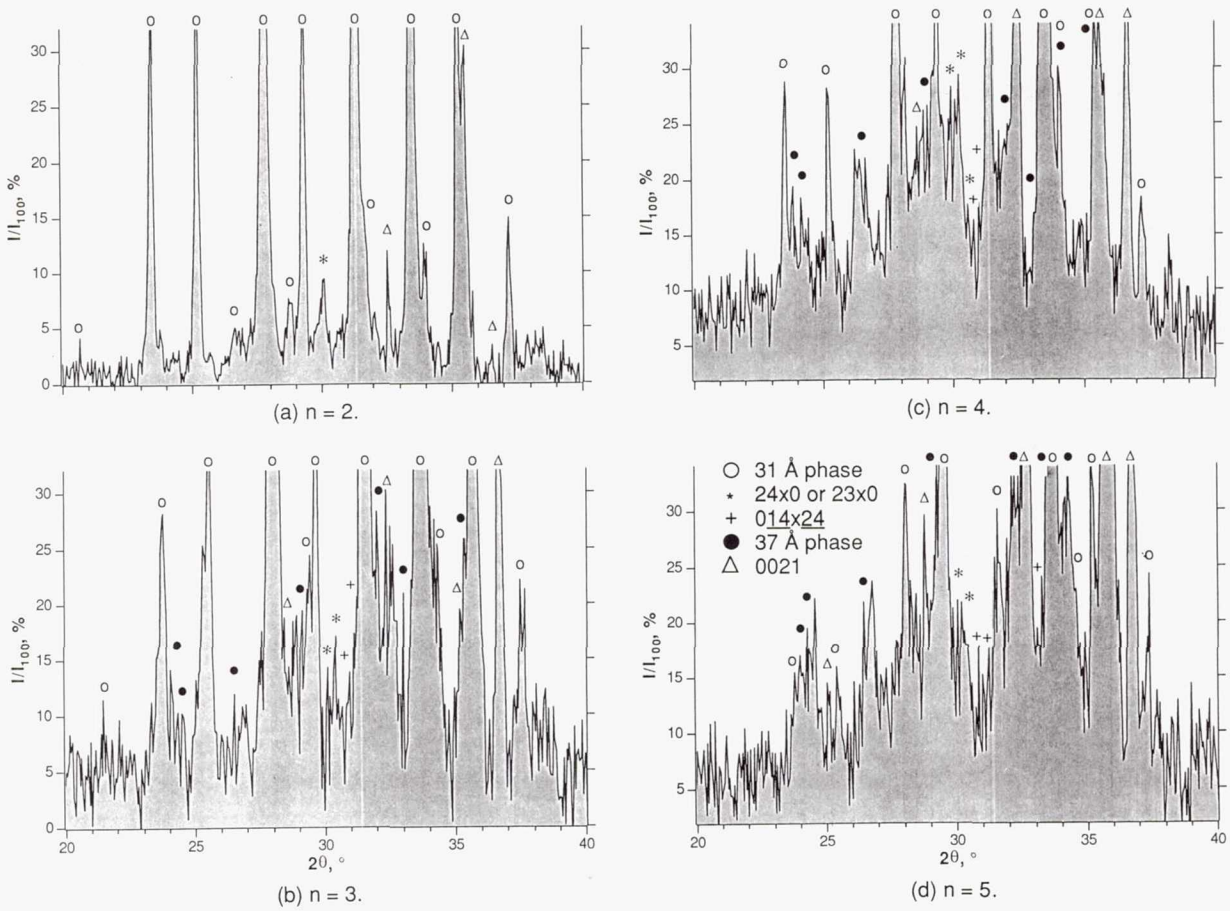

Figure 5.—XRD patterns of $Bi_2Sr_2Ca_{n-1}Cu_nO_z$ samples heated at 870 °C for 470 hr (Cu K_α radiation).

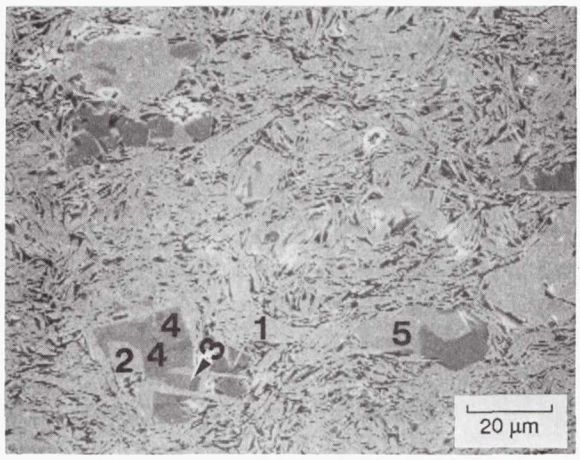

(a) n = 2.

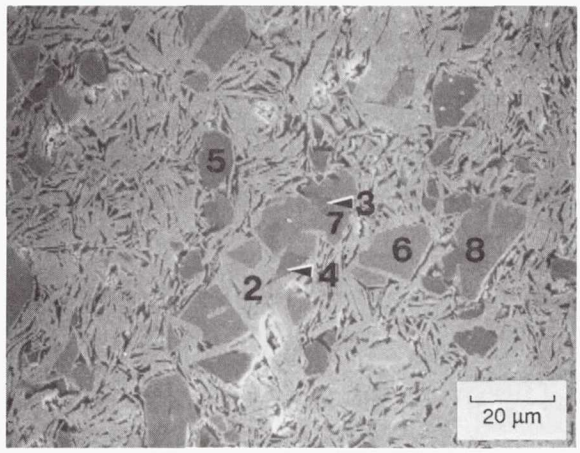

(b) n = 3.

Figure 6.—SEM photographs of samples heated at 870 °C for 470 hr. Compositions of the numbered regions are listed in Table II. The light matrix phase is the superconductor; the medium gray phase is 0$\underline{14}$x$\underline{24}$ and/ or CuO; the dark gray phase is Ca_2 CuO_{3+z}; and the black regions are porosity.

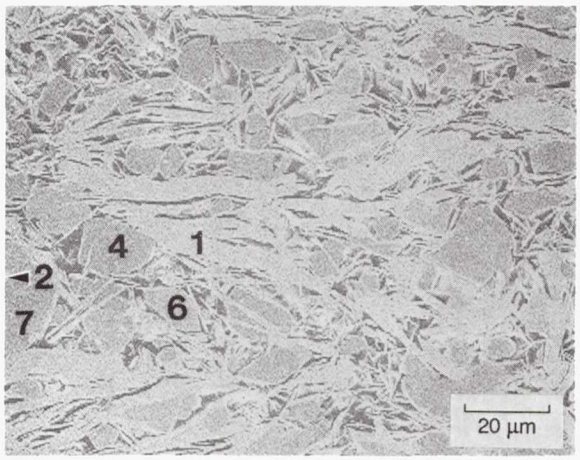

(c) n = 5.

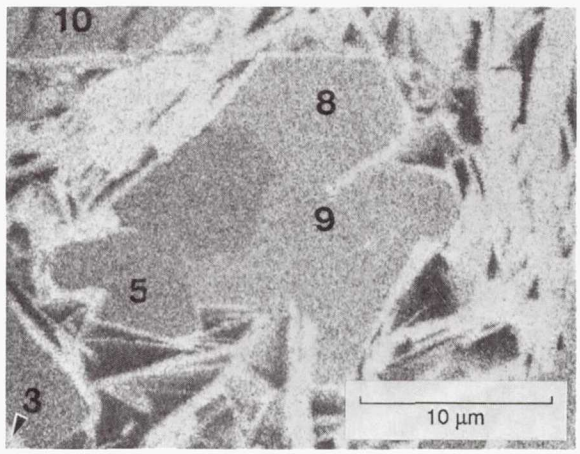

(d) n = 5.

Figure 6.—Concluded.

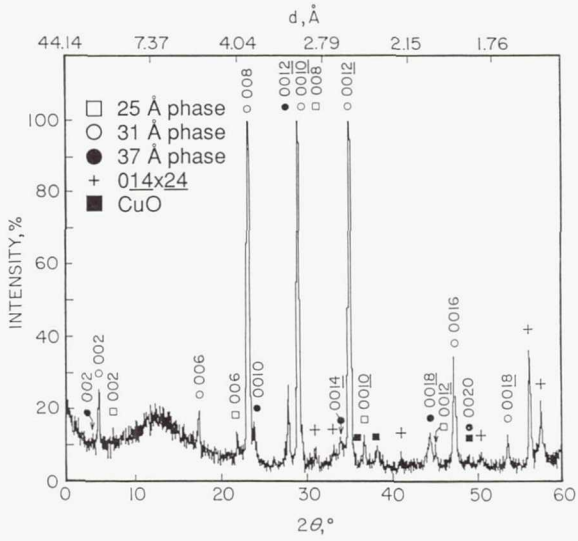

Figure 7.—Powder XRD pattern of n = 5 sample (870 °C/70 hr, 850 °C/15 hr) after magnetic alignment at room temperature in a field of 9.4 T.

NASA
National Aeronautics and Space Administration

Report Documentation Page

1. Report No.	2. Government Accession No.	3. Recipient's Catalog No.
NASA TM-103749		

4. Title and Subtitle

The Series $Bi_2Sr_2Ca_{n-1}Cu_nO_{2n+4}$ $(1 \leq n \leq 5)$: Phase Stability and Superconducting Properties

5. Report Date

6. Performing Organization Code

7. Author(s)

Mark R. De Guire, Narottam P. Bansal, David E. Farrell, Valerie Finan, Cheol J. Kim, Bethanie J. Hills, and Christopher J. Allen

8. Performing Organization Report No.
E-6000

10. Work Unit No.
307-51-00

9. Performing Organization Name and Address

National Aeronautics and Space Administration
Lewis Research Center
Cleveland, Ohio 44135-3191

11. Contract or Grant No.

13. Type of Report and Period Covered
Technical Memorandum

12. Sponsoring Agency Name and Address

National Aeronautics and Space Administration
Washington, D.C. 20546-0001

14. Sponsoring Agency Code

15. Supplementary Notes

Prepared for the 91st Annual Meeting of the American Ceramic Society, Indianapolis, Indiana, April 23-27, 1989. Mark R. De Guire, Case Western Reserve University, Cleveland, Ohio 44106 and NASA/ASEE faculty fellow at NASA Lewis Research Center; Narottam P. Bansal, NASA Lewis Research Center; David E. Farrell, Valerie Finan, Cheol J. Kim, Bethanie J. Hills, and Christopher J. Allen, Case Western Reserve University. Responsible person, Narottam P. Bansal, (216) 433-3855.

16. Abstract

Phase relations at 850 and 870 °C, and melting transitions in air, oxygen, and helium have been studied for $Bi_{2.1}Sr_{1.9}CuO_6$ and for the series $Bi_2Sr_2Ca_{n-1}Cu_nO_{2n+4}$ for $n = 1$, 2, 3, 4, 5, and ∞ (''$CaCuO_2$''). Up to 870 °C, the $n = 2$ composition resides in the compatibility tetrahedron bounded by $Bi_{2+x}(Sr,Ca)_{3-y}Cu_2O_8$, $(Sr,Ca)_{14}Cu_{24}O_{41}$, Ca_2CuO_3, and a Bi-Sr-Ca-O phase. The $n \geq 3$ compositions reside in the compatibility tetrahedron $Bi_{2+x}(Sr,Ca)_{3-y}Cu_2O_8 - (Sr,Ca)_{14}Cu_{24}O_{41} - Ca_2CuO_3 - CuO$ up to 850 °C. However, $Bi_{2+x}(Sr,Ca)_{4-y}Cu_3O_{10}$ forms for $n \geq 3$ after extended heating at 870 °C. $Bi_{2+x}Sr_{2-y}CuO_6$ and $Bi_{2+x}(Sr,Ca)_{3-y}Cu_2O_8$ melt in air at 914 °C and 895 °C respectively. During melting, all of the compositions studied lose 1-2% by weight of oxygen from the reduction of copper. $Bi_{2+x}Sr_{2-y}CuO_6$, $Bi_{2+x}(Sr,Ca)_{3-y}Cu_2O_8$ and $Bi_{2+x}(Sr,Ca)_{4-y}Cu_3O_{10}$ exhibit crystallographic alignment in a magnetic field, with the *c*-axes orienting parallel to the field.

17. Key Words (Suggested by Author(s))	18. Distribution Statement
Superconductors; Synthesis; Phase equilibria; Thermal analysis; Bismuth	Unclassified - Unlimited Subject Categories 76 and 27

19. Security Classif. (of this report)	20. Security Classif. (of this page)	21. No. of pages	22. Price*
Unclassified	Unclassified	20	A03

*For sale by the National Technical Information Service, Springfield, Virginia 22161